

CALCULATION OF PARAMETERS OF A CYLINDRICAL HYDROGEN ELECTRIC ARC FROM GENERALIZED RELATIONSHIPS

A. F. Bubljevskii

UDC 537.523.5

Generalized expressions for various parameters of cylindrical arcs in hydrogen are presented. Results of calculations are compared with results of numerical and physical experiments.

Methods of physical and mathematical modeling are used in investigation of electric arcs. The physical modeling can manipulate categories of both original and generalized (complex and parametric) variables. In the latter case the theory of similarity and dimensions is involved. The essence of each experiment, including those manipulating original variables, is modeling, since the object of the experiment is a particular model possessing necessary physical properties and corresponding to a certain extent to a natural object. The mathematical modeling of electric arcs, numerical or analytical, is carried out, as a rule, in terms of physical variables. In our recent work [1] we discuss problems of the analytical modeling of an arc discharge in terms of generalized quantities. The case of a cylindrical arc is considered when its dimensions and parameters do not vary along the channel.

The objective of the present work is a detailed analysis of results of generalized analytical modeling with hydrogen electric arcs taken as an example, in comparison with numerical and physical experiments carried out in terms of both simple and complex variables.

In order to obtain particular detailed relationships suitable for calculations of a hydrogen arc, one should analyze electro- and thermophysical properties of hydrogen and reconcile them with assumptions contained in a generalized model. In accordance with them, one should determine the proportionality coefficient in a linear approximation

$$Q = b_Q \Delta S, \quad (1)$$

and the proportionality coefficient and exponent in a power approximation

$$\sigma/\sigma_0 = (\Delta S/\Delta S_0)^{n_\sigma}. \quad (2)$$

Calculation of the thermal conductivity potential $S = \int_0^T \lambda dT$ preceding the above procedure is complicated by inconsistency of the published data on the $\lambda(T)$ dependence.

A rather complete calculation of transfer coefficients in hydrogen has been carried out in [2]. Among those, the dependences of interest, $\sigma(T)$ and $\lambda(T)$, can be found as determined within the region of variations of $T = (5-50) \cdot 10^3$ K and $P = 0.001, 0.01, 0.1, 1.0$ MPa. Comparison of various experimental data in cascade arcs [3] has shown that experimental values of λ exceed substantially – by more than twofold – theoretical estimates [2] within the wide region $T \approx (5-26) \cdot 10^3$ K at $P = 0.1$ MPa. The same picture was revealed in [4].

The problem of the discrepancy between theory and experiment for the thermal conductivity of hydrogen is discussed in [5]. Investigations [6, 7] measuring λ in both hydrogen and deuterium plasmas have shown that the above-mentioned discrepancy can be explained by a deviation of the ionization degree from the equilibrium value at the arc periphery at $T < 16,000$ K, which can result from diffusion of charged particles. It is pointed out

Academic Scientific Complex "A. V. Luikov Heat and Mass Transfer Institute of the Academy of Sciences of Belarus, Minsk, Belarus." Translated from *Inzhenerno-Fizicheskii Zhurnal*, Vol. 70, No. 4, pp. 569-575, July-August, 1997. Original article submitted February 2, 1997.

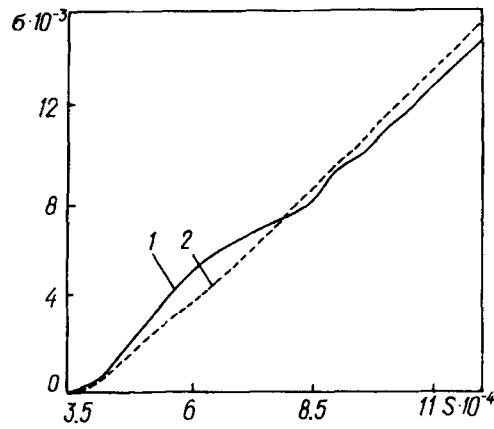


Fig. 1. Approximation of the dependence of the electric conductivity of hydrogen on the thermal conductivity potential: 1) combined theoretical and experimental dependence based on data from [2, 3, 5-10]; 2) power approximation $\sigma = 2.47 \cdot 10^{-2} \Delta S^{1.176}$, $P = 0.1$ MPa. σ , $(\Omega \cdot m)^{-1}$, S , W/m.

[5] that the measured λ is an effective value, since it depends on the configuration of the plasma volume and temperature gradient. Introduction of a correction for the nonequilibrium composition makes it possible to reconcile experimental results with calculations. However, the situation is not completely clear at $T > 16,000$ K, where an unexplained discrepancy of the theory [2] from experimental data [8-10] is observed, as is a discrepancy of the latter from the experiment [5-7], which under these conditions agrees with the calculations [2].

The above analysis resulted in constructing the $\lambda(T)$ function from data by various authors. In the region of $T = (2-5) \cdot 10^3$ K, the data [8] were taken due to their uniqueness. In other temperature ranges, coincidence of experimental or theoretical data from two or three groups of sources was taken as a selection criterion. In the region $T = (8-16) \cdot 10^3$ K we chose data by Asinovskii [5] and Nizovskii et al. [6, 7], who experimentally substantiated and explained the excess of λ over its theoretical value which was observed in [8-10]. For the region $T = (16-25) \cdot 10^3$ K, we can recommend data from [2], since, according to [5-7], the experimental data agree within the interval with the calculation for equilibrium conditions presented in [2]. Integration of the resultant curve over the entire region $T = (2-25) \cdot 10^3$ K yielded the required $S(T)$ dependence.

The quantity S_* entering into ΔS on the boundary of the conducting zone was determined beforehand from a linear approximation of the $\sigma(S)$ dependence by the method of least squares. On doing this, the same method was used to process data in the form (1), (2). The averaged experimental dependence $\sigma(T)$ [3], built with the use of results from [9, 10] and other works and very close to results of calculations [2], was used as an initial approximation for the region $T = (7-25) \cdot 10^3$ K. In this case, as has been noted in [3], results from [10] should be corrected for errors in evaluation of the temperature.

Data on the bulk radiation density were taken from [11] for an arc radius of 1 cm within the limits $T = (7-20) \cdot 10^3$ K.

The approximating dependence (2) is shown in Fig. 1 along with the original combined theoretical and experimental dependence.

Parameters of the approximation are presented in Table 1.

By substituting numerical values for hydrogen from the Table into formulas presented in [12], one can obtain the following dimensionless relationships for the hydrogen-arc parameters:

$$\bar{r}_* = \exp \left[(-2.212 K_S \left(\frac{Po}{\bar{r}_*^2 (1 + 0.17 K_Q \bar{r}_*^2)} \right)^{-0.459} \right], \quad (3)$$

$$\overline{\Delta S}_I(\bar{r}) = 0.361 \left(\frac{Po}{\bar{r}_*^2 (1 + 0.17 K_Q \bar{r}_*^2)} \right)^{0.459} J_0(2.4 \bar{r} / \bar{r}_*), \quad (4)$$

TABLE 1. Original and Approximation Parameters of Thermo- and Electrophysical Properties of Hydrogen, $P = 0.1$ MPa

Parameter	Dimension	Parameter value	Parameter	Dimension	Parameter value
T (range of variation)	10^3 K	2–25	ΔS_0	10^4 W/m	1.158
T_*	10^3 K	7.1	σ_0	$10^3 (\Omega \cdot \text{m})^{-1}$	1.494
S_*	10^4 W/m	3.542	n_σ	–	1.176
T_1	K	600	k_σ	–	0.865
S_1	W/m	150	$1/(n_\sigma + 1)$	–	0.459
ΔS_1	10^4 W/m	–3.523	$n_\sigma/(n_\sigma + 1)$	–	0.541
T_0	10^3 K	10	b_Q	–	2.874

$$\overline{\Delta S_{II}}(\bar{r}) = K_S \frac{\ln(\bar{r}/\bar{r}_*)}{\ln(1/\bar{r}_*)}, \quad (5)$$

$$\Pi_E = 2.834\bar{r}_*^{-2} \left(\frac{\text{Po}}{\bar{r}_*^2 (1 + 0.17K_Q \bar{r}_*^2)} \right)^{-0.541}, \quad (6)$$

$$\Pi'_E = 8.023 \bar{r}_*^{-2} (1 + 0.17K_Q \bar{r}_*^2) \left(\frac{\text{Po}}{\bar{r}_*^2 (1 + 0.17K_Q \bar{r}_*^2)} \right)^{-0.0811}, \quad (7)$$

$$\Pi_N = 2.828 (1 + 0.17K_Q \bar{r}_*^2) \left(\frac{\text{Po}}{\bar{r}_*^2 (1 + 0.17K_Q \bar{r}_*^2)} \right)^{0.459}, \quad (8)$$

$$\Pi_q = 0.452 \left(\frac{\text{Po}}{\bar{r}_*^2 (1 + 0.17K_Q \bar{r}_*^2)} \right)^{0.459}. \quad (9)$$

The same expressions can be written in dimensional form with the help of Table 1:

$$\bar{r}_* = \exp \left[-1.426 \cdot 10^4 (1 + 4.97 \cdot 10^4 R^2 \bar{r}_*^2)^{0.459} \left(\frac{I}{R\bar{r}_*} \right)^{-0.919} \right], \quad (10)$$

$$\Delta S_I(\bar{r}) = 1.97 (1 + 4.97 \cdot 10^4 R^2 \bar{r}_*^2)^{-0.459} \left(\frac{I}{R\bar{r}_*} \right)^{0.919} J_0(2.4\bar{r}/\bar{r}_*), \quad (11)$$

$$\Delta S_{II}(\bar{r}) = 3.523 \frac{\ln(\bar{r}/\bar{r}_*)}{\ln \bar{r}_*}, \quad (12)$$

$$ER = 15.503\bar{r}_*^{-1} (1 + 4.97 \cdot 10^4 R^2 \bar{r}_*^2)^{-0.541} \left(\frac{I}{R\bar{r}_*} \right)^{-0.0811}, \quad (13)$$

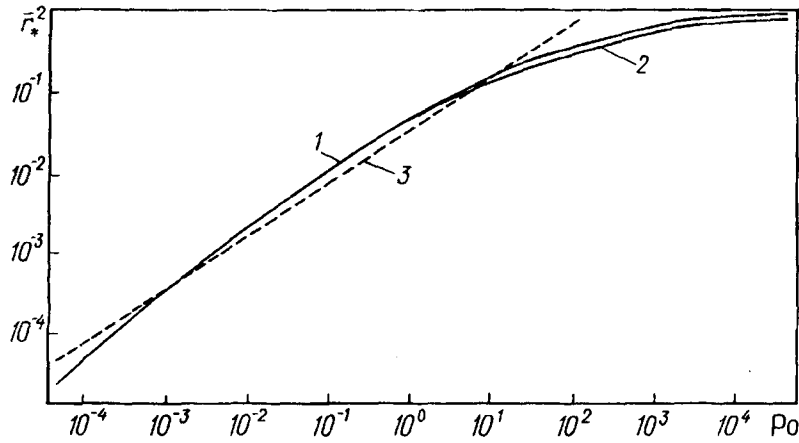


Fig. 2. Dependence of the squared dimensionless radius of the electroconductivity zone of the hydrogen arc on the number Po : 1) calculation without taking into account radiation, $R \rightarrow 0$; 2) calculation taking radiation into account, $R = 5$ mm; 3) power approximation of the curve 1: $\bar{r}_*^2 = 3.21 \cdot 10^{-2} Po^{0.649}$; $P = 0.1$ MPa.

$$qR = 2.473 (1 + 4.97 \cdot 10^4 R^2 \bar{r}_*^2)^{-0.459} \left(\frac{I}{R \bar{r}_*} \right)^{0.919}, \quad (14)$$

$$EI = 15.503 (1 + 4.97 \cdot 10^4 R^2 \bar{r}_*^2)^{0.541} \left(\frac{I}{R \bar{r}_*} \right)^{0.919}. \quad (15)$$

The dimensional coefficients are presented in SI units. For convenience, the relative quantities \bar{r} and \bar{r}_* are used. Equation (7), which is equivalent to (6), is reduced to (13).

From Eqs. (3), (6), and (10), (13) one can obtain very convenient expressions for calculation of the volt-ampere characteristic (VAC) of an arc in parametric form, where the arc radius \bar{r}_* is used as a parameter:

$$Po = 5.642 \bar{r}_*^2 (1 + 0.17 K_Q \bar{r}_*^2) \left(\frac{K_S}{\ln(1/\bar{r}_*)} \right)^{2.176}, \quad (16)$$

$$\Pi_E = 1.112 \bar{r}_*^{-2} \left(\frac{\ln(1/\bar{r}_*)}{K_S} \right)^{1.176}, \quad (17)$$

$$\frac{I}{R} = \bar{r}_* \left(\frac{7.014 \cdot 10^{-5} \ln(1/\bar{r}_*)}{1 + 4.97 \cdot 10^4 R^2 \bar{r}_*^2} \right)^{-1.088}, \quad (18)$$

$$ER = 6.66 \bar{r}_*^{-1} \sqrt{1 + 4.97 \cdot 10^4 R^2 \bar{r}_*^2} (\ln(1/\bar{r}_*))^{0.088}. \quad (19)$$

Figure 2 presents the dependence of the squared dimensionless arc radius on the Po number calculated by expression (16). Calculations have shown that for $Po < 5.2 \cdot 10^1$ ($I/R < 3 \cdot 10^4$ A/m) the neglect of radiation for a radius of 5 mm leads to an error in evaluation of the radius of the conducting zone not exceeding 6%. In addition, since $\bar{r}_*^2 = 1$ is a horizontal asymptote of the curve $\bar{r}_*^2 = f(Po)$, the quantities \bar{r}_*^2 and \bar{r}_* can be assumed to equal unity at large Po within a considerable range of variations of this quantity.

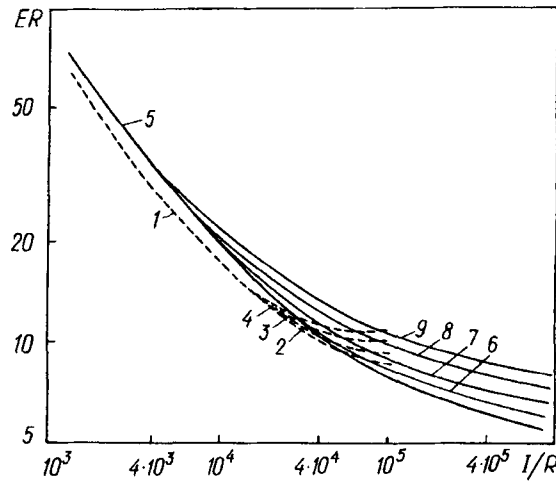


Fig. 3. Comparison of analytical and numerical calculations of channel radius-scaled $E-I$ characteristics of cylindrical hydrogen arc: 1-4) numerical calculation [11], 5-9) calculation by generalized dependences; 1, 5) without taking radiation into account; 2-4), 6-9) taking radiation into account; $R = 2$ (2, 6), 3 (3, 7), 4 (4, 8), and 5 mm (4). $P = 0.1$ MPa. ER , V; I/R , A/m.

A numerical analysis of a cascade hydrogen arc with allowance for radiation transfer has been carried out in [11]. Figure 3 presents a comparison of these calculations with analytical results in $ER = f(I/R)$ coordinates by expressions (18) and (19). It is evident that a considerable fibering of this parameter over the channel radius begins at $I/R = 4 \cdot 10^3$ A/m, whereas in numerical calculations the fibering becomes noticeable at $I/R > 2 \cdot 10^4$ A/m. At this I/R value the error resulting from neglecting radiation in the analytical calculation within the same range of variations of R is 10%. As a whole, the analytical $E-I$ characteristic follows the numerical one but exceeds it by at most 15%, up to $Po \approx 5 \cdot 10^4$. An empirical correction of coefficients in (16)-(19) can improve substantially the agreement of the methods.

An experimental verification of calculations was carried out on the basis of results from [3], which presents results of an experiment where I/R changes by almost four orders of magnitude. In this case, ER changes by more than two orders of magnitude. The dimensionless numbers Po and Π'_E change by almost eight and more than four orders of magnitude, respectively. The experiments were carried to provide a decrease in the current with an increasing channel radius, and vice versa. As a result, radiation from the column was minimum and, as follows from estimations, it can be neglected. Figure 4, which illustrates this comparison, presents also results of a numerical simulation [11] and analytical calculation [3]. It is evident that an analytical calculation by expressions (3) and (7) agrees with results of numerical calculation and experiment in the logarithmic coordinates $\Pi'_E = f(Po)$ when radiation is neglected. The theoretical dependence is presented by a curve in these coordinates. The difference in the main portion of the generalized curve does not exceed $\pm 60\%$, and $\pm 26\%$ for the quantity ER . The discrepancy of the curves in the left portion of the figure, reaching -150% (and -60% for ER), is explained in [3] by nonequilibrium phenomena at low currents and high field strengths. The position of the discrepancy region depends on the channel radius. A deviation from the local thermodynamic equilibrium (LTE) means that a higher electron temperature causes the conductivity to exceed its equilibrium value. In this case the field strength does not increase at a rate that can be achieved under conditions of LTE with decreasing current.

In physical modeling, the form of the generalized characteristic is usually preset by a product of functions of each of the generalized arguments

$$\Pi_i = C_i \prod_{n=1}^N F_{ni}(K_{ni}). \quad (20)$$

It is usually assumed that $F_{ni}(K_{ni}) = A_{ni} K_{ni}^{\alpha_{ni}}$; therefore, (20) takes the form of a product of separate power functions

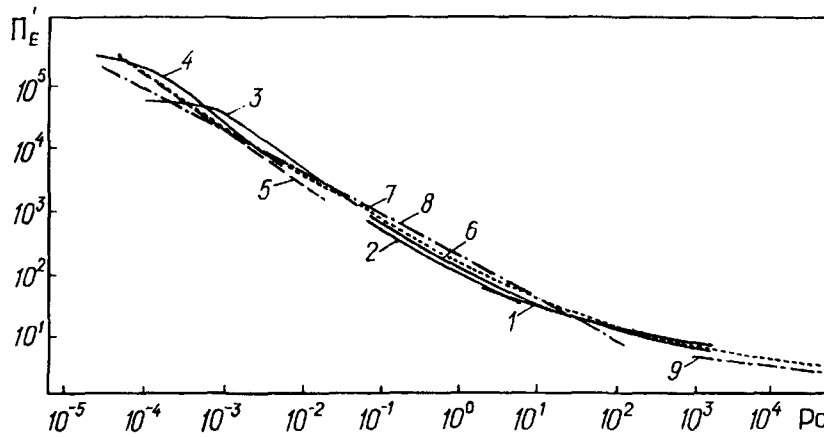


Fig. 4. Generalized differential volt-ampere characteristic of cylindrical hydrogen arc: 1-4) experimental data presented in [2]; $R = 1$ (1), 2.5 (2), 9.25 (3), and 20 mm (4); 5) calculation [3]; 6) numerical calculation [11], $R \rightarrow 0$; 7) calculation by generalized dependences, $K_Q = 0$; 8) power approximation $\Pi'_E = 1.891 \cdot 10^2 Po^{-0.677}$; 9) power approximation $\Pi'_E = 3.023 Po^{-0.081}$; $P = 0.1$ MPa.

$$\Pi_i = A_i \prod_{n=1}^N K_{ni}^{\alpha_{ni}}. \quad (21)$$

This choice is not substantiated by any reason except for convenience. The convenience consists in the fact that a power function is presented by a straight line in logarithmic coordinates, and expressions (20), (21) can always be reduced to a function of a single generalized variable and be presented graphically by a straight line, which is pictorial. The form (20) is used, in, e.g., [13], and expression (21) is used in [14].

Analytical formulas (3), (4), and (6)-(9) cannot be reduced in the general case to the form (20), (21) even for a single gas. This possibility appears only in certain particular cases. In view of the fact that, according to (3), $\bar{r}_* \rightarrow 1$ when $Po \rightarrow \infty$, for large values of the Po number one can approximately set $\bar{r}_* = 1$, as has been already mentioned. Then expressions (3), (6), and (6)-(9) take the form (20), and the form (21) for $K_Q \gg 1$. In the former case, as in the more general one $\bar{r}_* = \text{const}$, the dependence of Π'_E on Po in the form (20) can be presented by a single line in logarithmic coordinates, and the dependence on K_Q can be presented by a single curve. In the latter case, the form (21) is represented by a single line, irrespective of which of the quantities Po and K_Q is used as an argument.

Another particular case takes place when radiation is not taken into account, i.e., $K_Q \ll 1$ ($b_Q \rightarrow 0$ or $R \rightarrow 0$). Then $\bar{r}_*^2 = f(Po)$ can be approximated by a power function, which, upon its substitution in, e.g., expressions (6) or (7) for Π_E or Π'_E at $K_Q \ll 1$ transforms then into simple power dependences on Po . Figure 2 illustrates the power approximation of $\bar{r}_*^2 = f(Po)$ for hydrogen. In this case it can be written in the form

$$\bar{r}_*^2 = 3.21 \cdot 10^{-2} Po^{0.649}. \quad (22)$$

The formula holds within the region of $Po = 5 \cdot 10^{-4} - 10^2$.

By substituting (22) into (7) at $K_Q = 0$, we obtain

$$\Pi'_E = 1.891 \cdot 10^2 Po^{-0.677}. \quad (23)$$

Figure 4 presents an approximation of the $\Pi'_E = f(Po)$ curve calculated using expressions (3) and (7) at $K = 0$, by the power function (23) within the range of $Po = 5 \cdot 10^{-4} - 10^2$. Also presented is dependence (7) which transforms into

$$\Pi'_E = 8.023 \text{Po}^{-0.081} \quad (24)$$

at $K_Q = 0$ and $\bar{r}_* = 1$.

It is evident that the difference between approximation (23) and the "exact" curve at the ends of the interval $\text{Po} = 5 \cdot 10^{-4} - 10^2$ reaches -60% or -26% for the quantity $\sqrt{\Pi'_E} \sim ER$. The same picture is observed also for approximation (22) at $\text{Po} = 10^3$. In the main portion of the curve in the former case and at the end of the interval $\text{Po} = 2 \cdot 10^4$ in the latter, this difference is $\sim 26\%$ for the quantity Π'_E and $\sim 12\%$ for the quantity ER .

Thus, we have found as a result of the analysis of methods of physical and generalized modeling that forms of empirical and analytical dependences even for a single gas correspond to each other only in certain particular cases ($\bar{r}_* = \text{const}$ or $\bar{r}_* = \text{var}$ according to a power law in combination with $K_Q \gg 1$ or $K_Q \ll 1$).

The use of the "exact" rather than the power law of variation of the column radius in calculations leads to bending of the generalized differential VAC of the arc in coordinates $\log \Pi'_E = f(\log \text{Po})$, and taking into account of radiation in a volume approximation leads to fibering over the channel radius. The results of calculations and experiment agree satisfactorily.

NOTATION

σ , electric conductivity; λ , thermal conductivity; T , temperature; P , pressure, E , electric field strength; I , current strength; r , running radius; R , channel radius; Q , bulk radiation density; q , thermal flux density; $S = \int_0^T \lambda dT$, thermal conductivity potential; $\bar{r} = r/R$; $\Delta S = S - S_*$; $\overline{\Delta S} = \Delta S / \Delta S_0$; J_0 , Bessel function; Π_i , K_{ni} , $\text{Po} = I^2 / R^2 \sigma_0 \Delta S_0$, $K_Q = Q_0 R^2 / \Delta S_0$; $K_S = -\Delta S_1 / \Delta S_0$, $\Pi_E = ER^2 \sigma_0 / I$, $\Pi'_E = E^2 R^2 \sigma_0 / \Delta S_0$, $\Pi_N = EI / \Delta S_0$, $\Pi_q = q_1 R / \Delta S_0$, dimensionless similarity numbers; n_σ , α_{ni} , exponents; $b_Q = Q_0 / \Delta S_0$. Subscripts: *, boundary of conducting zone; 0, governing value; 1, value at the wall; I, II, conducting and nonconducting zones, respectively.

REFERENCES

1. A. F. Bublichskii, *Inzh.-Fiz. Zh.*, **70**, No. 1, 99-104 (1993).
2. R. S. Devoto, *J. Pl. Phys.*, **2**, No. 4, 617-631 (1968).
3. G. Mekker and W. Bauder, in: *Properties of Low-Temperature Plasma and Methods for Its Diagnostics* [in Russian], Novosibirsk (1979), pp. 37-56.
4. W. Plantikov and S. Steinberger, *Z. Phys.*, **231**, H.2, 109-119 (1970).
5. E. I. Asinovskii, in: *Properties of Low-Temperature Plasma and Methods for Its Diagnostics* [in Russian], Novosibirsk (1977), pp. 57-65.
6. V. L. Nizovskii and V. I. Shabashov, *Teplofiz. Vys. Temper.*, **11**, No. 9, 251-255 (1973).
7. V. L. Nizovskii, K. A. Khodakov, and V. I. Shabashov, *Teplofiz. Vys. Temper.*, **11**, No. 6, 1287-1289 (1973).
8. K. Behringer, W. Kollmar, and J. Mentel, *Z. Phys.*, **215**, H. 2, 127-151 (1968).
9. H. Motschmann, *Z. Phys.*, **191**, H. 1, 10-23 (1966).
10. S. Steinberger, *Z. Phys.*, **233**, H. 1, 1-18 (1969).
11. V. H. Vetlutskii, A. G. Onufriev, and V. G. Sevast'yanenko, in: *Low-Temperature Plasma* [in Russian], Moscow (1967), pp. 395-407.
12. A. F. Bublichskii and O. I. Yas'ko, in: *Proceedings of TPP-3, Aachen, Germany, September 19-21, 1994, Aachen* (1995), pp. 267-272.
13. G. Yu. Dautov and M. I. Sazonov, in: *Low-Temperature Plasma Generators* [in Russian], Moscow (1969), pp. 200-208.
14. A. I. Zhidovich, S. K. Kravchenko, and O. I. Yas'ko, in: *Low-Temperature Plasma Generators* [in Russian], Moscow (1969), pp. 200-208.